The σ-IASI-β

Giuseppe Grieco, Carmine Serio and Guido Masiello

University of Basilicata, School of Engineering, Potenza, Italy; giuseppe.grieco@gmail.com; carmine.serio@unibas.it; guido.masiello@unibas.it

Abstract. This paper describes an improved, faster, implementation of the σ-IASI model, with a new parameterization of radiative transfer in cloudy atmosphere. The model can compute up and/or down-welling spectral radiances, emitted from the earth's system and their analytical Jacobians with respect to a set of geophysical parameters and the water vapor and carbon dioxide continua absorbing coefficients. The paper presents also its software implementation and a retrieval exercise of the tropospheric content of CO2, CO, N2O and CH4 on the Mediterranean Sea. The content of the gases is compared with the ground based measurements of the Global Atmosphere Watch network. The innovation introduced in the model is the down-sampling of the look-up table by means of a spectral averaging of the layer optical depths on bins of 10−2 cm−1 width before they are parameterized as a low order polynomial of temperature and, only for water vapor, of water vapor concentration itself to take into account the self-broadening effect. The down-sampling of the look-up table is responsible for an additional speed-up which makes the code useful for almost real time retrieval applications and thus useful for operational purposes. This code is a powerful tool also to check the validity of the molecular spectroscopic parameters. The code is an evolution of the well-known code σ-IASI. It has been developed in the context of the Infrared Atmospheric Sounding Interferometer (IASI) of the European Space Agency EUMETSAT but it is well suited for every nadir viewing satellite, airplane sensor or ground-based sensor with a sampling rate in the range 0.1-2 cm-1.

Keywords. Spectroscopy, Interferometry, Infrared, Remote Sensing, FTS-PSI.

1. Introduction

Humidity and temperature have been identified as major variables in assessing climate change and they play a fundamental role in Earth's energy and water cycle processes. An accurate knowledge of also the minor and trace gases plays a fundamental role in the comprehension of the climate. It is now recognized that the current spectral resolution of modern hyper-spectral sensors (≈ 0.5 cm-1) meets the specifications issued by the World Meteorological Organization (WMO) on accuracy needed to improve weather forecasts (temperature with an average error of 1 K; humidity with an average error of 10%-20%; vertical resolution of 1 Km, at least in the lower troposphere).

Such of these instruments are the American Advanced Infrared Radiometer Sounder (AIRS)(Aumann et al., 2003 [1]) which flies on board the polar orbiting satellite platform AQUA issued by NASA and the European Infrared Atmospheric Sounding Interferometer (IASI) (Cayla, 1995) [2] which flies on board the polar orbiting satellite platform MetOp issued by EUMETSAT.

The accuracy of the knowledge of the thermodynamic state of the atmosphere and of the minor and trace gases depends firstly on the quality of the observations, but also on the strategy adopted for the retrieval of the geophysical parameters. Physical based inversion methods have largely demonstrated to be the most accurate (Masiello et al. 2009) [3] even if, on the other hand, they are not competitive from a time performance point of view. This aspect poses a strong limit to the full exploitation of all the available observations. To have an idea of the burden of the available high spectral resolution observations, consider that IASI is able to measure 120 radiance spectra every 8

seconds and this burden will further increase with the Meteosat Third Generation mission. Consequently, an inverse tool should be able to retrieve the thermodynamic state of the atmosphere and minor and trace gases in less than one second.

The core of an inverse tool is the direct radiative transfer model and it is also the most time demanding part of the process. This is the reason why so many different strategies have been developed in order to approximate the computation of the radiance spectrum and its derivatives with respect to the geophysical parameters.

This paper fully describes an hyper-fast monochromatic radiative transfer model designed for research and operational computation of either clear sky and cloudy spectral radiance, its analytical derivatives (Jacobians) with respect to a given set of geophysical parameters and the absorbing coefficients of the continua of H2O and CO2 and its software implementation. It is an evolution of the well-known σ-IASI code. It is based on a down-sampled look-up table of pre-computed optical depths and has been designed for every instrument which sounds the emitted spectrum of the Earth in the spectral range from 0 to 2800 cm-1 with a sampling rate between 0.1 and 2 cm-1 for nadir viewing satellite and air-borne sensors and for ground-based sensors. The code is expected to provide the needed accurate forward model calculation for meteorological and climate application in order to retrieve the thermodynamic state of the atmosphere and the tropospheric concentration of trace and minor gases. Finally, it can be used in radiance closure studies to assess the consistency of the spectroscopic parameters (Masiello et al. 2009 [3]).

An application of the code with the purpose of retrieving the tropospheric concentration of CO2, CO, CH4 and N2O over the whole Mediterranean Sea for the month of July 2010 is presented and discussed. The retrieved values are then compared with the in situ ground based measurements of the Global Atmosphere Watch network.

2. Methods

2.1. Optical depth down-sampling methodology

The basic ingredients to compute the spectral radiance and its Jacobians with respect to the geophysical parameters are a) the thermodynamic state of the atmosphere and the vertical concentration profile of all the chemical species (atmospheric profile) and b) the monochromatic layer optical depth. The monochromatic layer optical depth depends itself on the atmospheric profile. The generation of the monochromatic layer optical depth is the most time demanding part of the code. The basic idea to speed-up the code is to compute only once the layer optical depth and then store it in a suitable lookup table (Amato et al., 2002 [4]).

The innovation introduced here is the down-sampling of the layer optical depth lookup table. For each species (h) we can define an equivalent optical depth $\chi^{(h)}_{<\nu>}$ that can be parameterized with respect to temperature (and with respect to water vapor mixing ratio for the only case of the water vapor to take into account the self-broadening effect [5]). With the symbols $\langle\cdot\rangle$ we indicate the average operation over the spectral range identified by the coarse resolution. Given that $q^{(h)}_j$ is the mass mixing ration of the (h)-th species and T_j is the physical temperature of the j-th atmospheric layer, the equivalent optical depth will be

$$\chi^{(h)}_{<\nu>,j} = q^{(h)}_j \left(c^{(h)}_{<\nu>,0j} + c^{(h)}_{<\nu>,1j} T_j + c^{(h)}_{<\nu>,2j} T_j^2 \right)$$

where the equivalent coefficients $c^{(h)}_{<\nu>,kj}$ with k = 0, 1, 2, are obtained by fitting the layer transmittance averaged over the coarse resolution

$$q_j^{(h)}\left(c_{<\nu>,0\,j}^{(h)} + c_{<\nu>,1j}^{(h)} T_j + c_{<\nu>,2\,j}^{(h)} T_j^2\right) = -\log\left(\left\langle \tau_{\nu,j}^{(h)} \right\rangle\right) = -\log\left[\left\langle \exp\left(-\chi_{\nu,j}^{(h)}\right)\right\rangle\right]$$

For up-welling radiance, the optical depth of the j-th layer may be written as

$$\chi_j^{(h)} = -\log\left(\frac{\tau_{j-1}^{(h)}}{\tau_j^{(h)}}\right)$$

while for down-welling radiance it may be written as

$$\chi_j^{(h)} = -\log\left(\frac{\tau_j^{*(h)}}{\tau_{j-1}^{*(h)}}\right)$$

Here, for the (h)-th chemical species $\tau_j^{(h)}$ is the transmittance of the atmosphere from the top of the j-th layer to the top of the atmosphere, while $\tau_j^{*(h)}$ represents the transmittance of the top of the j-th layer to the bottom of the atmosphere and therefore, they obey to the relation

$$\tau_0^{(h)} = \tau_j^{(h)} * \tau_j^{*(h)}$$

The discretization of the atmosphere and the average process introduce some errors, therefore, the correct computation of the layer optical depth depends on the observation point. For the up-welling case, the layer optical depth is computed recursively from the top to the bottom of the atmosphere whilst the opposite happens for the down-welling case.

The monochromatic layer optical depth has been calculated by means of LBLRTM v12.1 (Clough et al., 1992 [6]) for a reference atmospheric state (US Standard Atmosphere 1962, Anderson et al., 1986 [7]) plus eight evenly spaced temperatures (±10K; … ; ±40K). The required spectroscopic parameters have been extracted from the database HITRAN 2008 (Rothman et al., 2009 [8])

2.2. Retrieval methodology

The retrieval algorithm for the trace gases CO2, CO, CH4 and N2O is based on the Fourier Transform Spectroscopy with Partially Scanned Interferogram technique (here-on FTS-PSI) and it uses the σ-IASI-β code as a subroutine.

The FTS-PSI has been applied in the recent past in order to retrieve the CO2 columnar content and the vertical mixing ratio (here-on VMR) of water vapor (Grieco et al., 2011 [9]) and for an optimal spectral data reduction for the assimilation of spectral informations in meteorological general circulation models (Grieco et al., 2010 [10]).

We apply a parametric retrieval of the VMR trace gas profile making the following hypothesis:

$$q(p) = q_0(p)(1 + f_q)$$

where $q(p)$ is the VMR profile to be retrieved, $q_0(p)$ is a suitable first guess reference VMR profile coming from the climatology and f is the parameter to be retrieved.

In (Lubrano et al., 2004 [11]) the authors show that a parametric and a non-parametric approach for the retrieval of the N2O tropospheric concentration are almost equivalent in terms of accuracy and degrees of freedom of the solution, the first one being faster. The retrieved quantity is representative of the tropospheric concentration of the gases. In fact, a) the sensitivity of the radiance to the trace gases concentration in the lowest layers of the atmosphere is very low, due to the poor thermal contrast between the sea surface and the lowest atmospheric layers and to the fact that the sea emissivity is very close to 1 (Lubrano et al., 2004 [11]) and b) the Jacobians do not have any sharp peak, all over their absorption spectral interval (we omit here for the sake of brevity) and it can be seen that the most of the contribution to Q comes from the part of the atmosphere between 200 and 700-800 mb.

Given that the final retrieved solution has just one degree of freedom, the only retrieved physical information concerns the total columnar content of the gas Q. It follows that the retrieved value Q is given by

$$Q = Q_0(1 + f_q)$$

where Q_0 is the total columnar content of the gas for the reference VMR profile.
The retrieval procedure for every trace gas goes through the following steps:

1. We produce a suitable first guess atmospheric state vector $\mathbf{v_0}$ coming from the simultaneous retrieval of T, T_s, water vapor and ozone by means of an optimal estimation retrieval algorithm as described in Masiello et al. 2009 ([3]) and from climatology for what concerns the trace gases.
2. We back-transform the observed radiance spectrum into the interferogram domain and select the proper optical path interval for the trace gas at hand (see Grieco et al., 2011 [9] for details concerning the FTS-PSI retrieval technique).
3. We assume that the true state vector $\mathbf{v}$ is scaled with respect to $\mathbf{v_0}$:
$$\mathbf{v_i} = \mathbf{v_{0i}}(1 + f_i)$$
where $\mathbf{v_i}$ stands for the final atmospheric state vector concerning the geophysical parameter i to be retrieved and f_i is the parameter to be retrieved. Here, the index i refers to the trace gas object of the retrieval and to any potentially interfering parameter retrieved with the optimal estimation algorithm (T, T_s, water vapor and ozone).
4. We produce a least square regression of $\mathbf{f}$ (whose components are f_i) directly in the interferogram domain by means of the following relation
$$\mathbf{f} = \left(\mathbf{A^t C^{-1} A}\right)^{-1} \mathbf{A^t C^{-1} \Delta I}$$
where $\mathbf{C^{-1}}$ is the observational error covariance matrix in the interferogram domain, $\mathbf{\Delta I}$ is the difference between the interferogram concerning the observed radiance spectrum and the interferogram concerning the first guess solution and $\mathbf{A}$ is the matrix of the Jacobians of the geophysical parameters which have a non negligible effect in the selected optical path interval multiplied by their initial guess state $\mathbf{v_0}$. All the potentially interfering parameters are expected to have a negligible variation, delimited by the precision of the optimal estimation retrieval. The intensity of this interfering effect is quantified by the index $\Delta_{\%}$ described later.
5. We estimate the accuracy of the method by computing the *a-posteriori* covariance matrix for the vector $\mathbf{f}$
$$\mathbf{S} = \left(\mathbf{A^t C^{-1} A}\right)^{-1}$$
From the error propagation law, we have that
$$\sigma_Q = \sigma_{f_q} Q_0$$
where σ_Q is the estimated accuracy of the trace gas content Q, σ_{fq} is the precision of the retrieved parameter f_q and Q_0 is the reference columnar content of the trace gas.
6. We assess the relative weight of the interfering geophysical parameters on the trace gas content by means of the index $\Delta_{\%}$:
$$\Delta_{\%} = \sum_{i=1}^{N-1} \left| f_i \right| * 100$$
where the index $i \neq N$ stands for every interfering parameter. $\Delta_{\%}$ is an *ad-hoc* index which measures the deviation of the final state vector from the optimal estimated solution for what concerns the interfering parameters. It follows that if $\Delta_{\%}$ is high, the final solution is too far from the initial guess for what concerns the interfering parameters previously retrieved, therefore the solution is not trustful. This deviation may be caused for example by a small cloud contamination. For what concerns the problem at hand, a suitable threshold value for

$\Delta_{\%}$ is 10, otherwise the complete solution is rejected. $\Delta_{\%}$ may be considered also a by-product of this method to be used as an *a-posteriori* quality check of the optimal estimation retrieval.

It must be remarked that the final state v is a solution only for what concerns the columnar content of the gas. For what concerns the parameters retrieved at the first retrieval step by means of the optimal estimation algorithm, the solution does not change.

The estimated accuracy of this methodology is resumed in table 1.

The estimated accuracy is referred to a single IASI pixel. The accuracy can be further improved by averaging with the neighboring pixels. IASI instantaneously acquires a 4 pixels matrix which lie in a box of around 50 Km side at nadir. Therefore, the estimated accuracy may be improved by a factor 2 given that the spacial resolution is decreased to about 50 Km at nadir.

Table 1. Estimated accuracy of the tropospheric content of the trace gases.

Chemical Species	**Estimated Accuracy**
CO_2	1%
CO	<1%
N_2O	4-5%
CH_4	1.5%

3. Results

The retrieval of the tropospheric content of the trace gases has been compared to the ground measurements of five Mediterranean stations of the Global Atmosphere Watch network and the data have been downloaded from the web site of the World Data Centre for Greenhouse Gases (http://ds.data.jma.go.jp/gmd/wdcgg/wdcgg.html). These stations are located in Begur (Spain), Finokalia (Greece), both owned by Laboratoire des Sciences du Climat et de l'Environnement de l'Institut Pierre Simone Laplace (LSCE/IPSL), Lampedusa (Italy), Sede Boker (Israel), both owned by Earth System Research Laboratory of the National Oceanic and Atmospheric Administration (ESRL/NOAA and another one in Lampedusa owned by the Italian National Agency for New Technologies, Energy and Sustainable Economic Development ENEA) and Cairo (Egypt), owned by the Egyptian Meteorological Authority (EMA). They span all the Mediterranean basin. The first three stations lie on the sea side, whilst the last two lie respectively at about 50 Km and 150 Km from the coast. The last two stations have been selected because they are the only available stations in the eastern Mediterranean basin. Figure 1 shows the location of the stations.

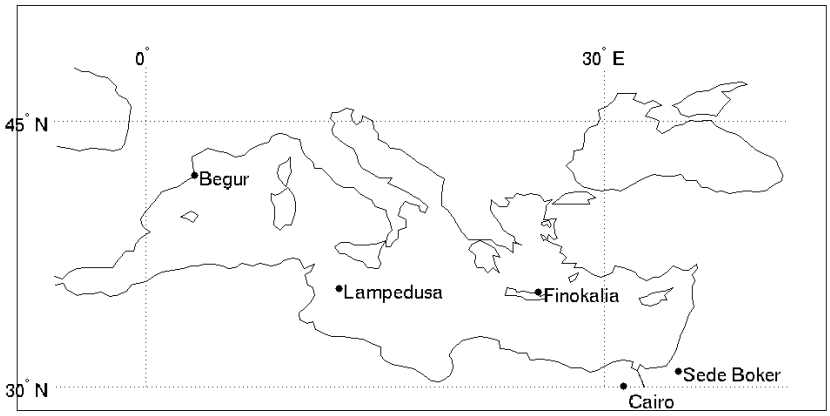

Figure 1. Location of the GAW stations.

Figure 2 shows the distribution of all the available clear sky IASI measurements for the period of July 2010.

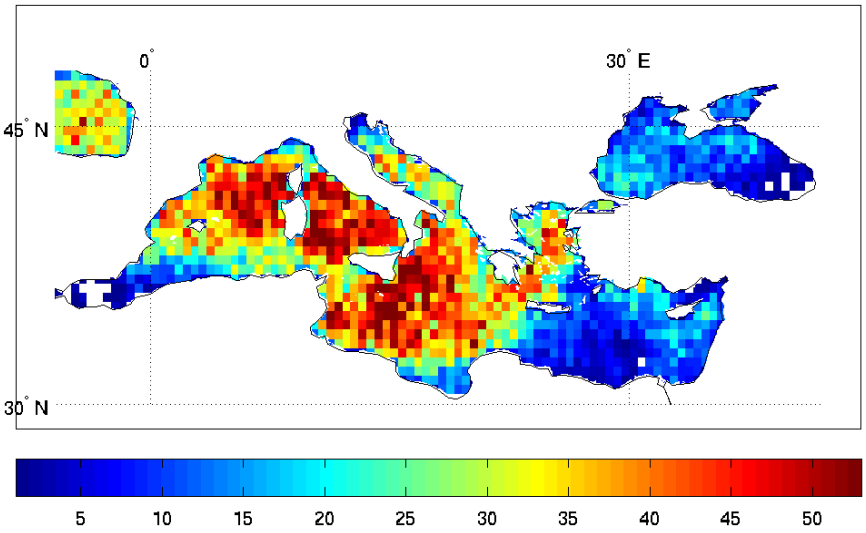

Figure 2. Spatial distribution of the available IASI measurements in bins of 0.5° x 0.5° latitude/longitude

The inhomogeneity of the distribution is due to the orbit characteristics of the satellite and to the cloud cover. We remark here that the platform is a polar orbiting satellite.

3.1. CO_2

The carbon dioxide has the largest radiative forcing (RF) among all the GHG. Even if it's radiative forcing power is lower than some other trace gases like N2O, the dependence of our life on fossil fuels, makes it one of the most alarming responsible of the greenhouse effect. A wide range of measurements confirm that the atmospheric mixing ratio of CO2 has increased by about 100 ppmv (36%) over the last 250 years, from a range of 275 to 285 ppmv in the pre-industrial era (AD 1000-1750) to 379 ppmv in 2005 and its average rate of increase is 1.4 ppmv yr-1 (IPCC 4th Assessment Report: Climate Change 2007).

Figure 3 shows the average tropospheric content of CO2 (parts per million of volume ppmv) over the Mediterranean basin during the month of July 2010. The field is smoothed with a low pass filter, which uses a pixel-wise adaptive Wiener filtering method based on statistics estimated from a local

neighborhood of each pixel, in order to emphasize the patterns.

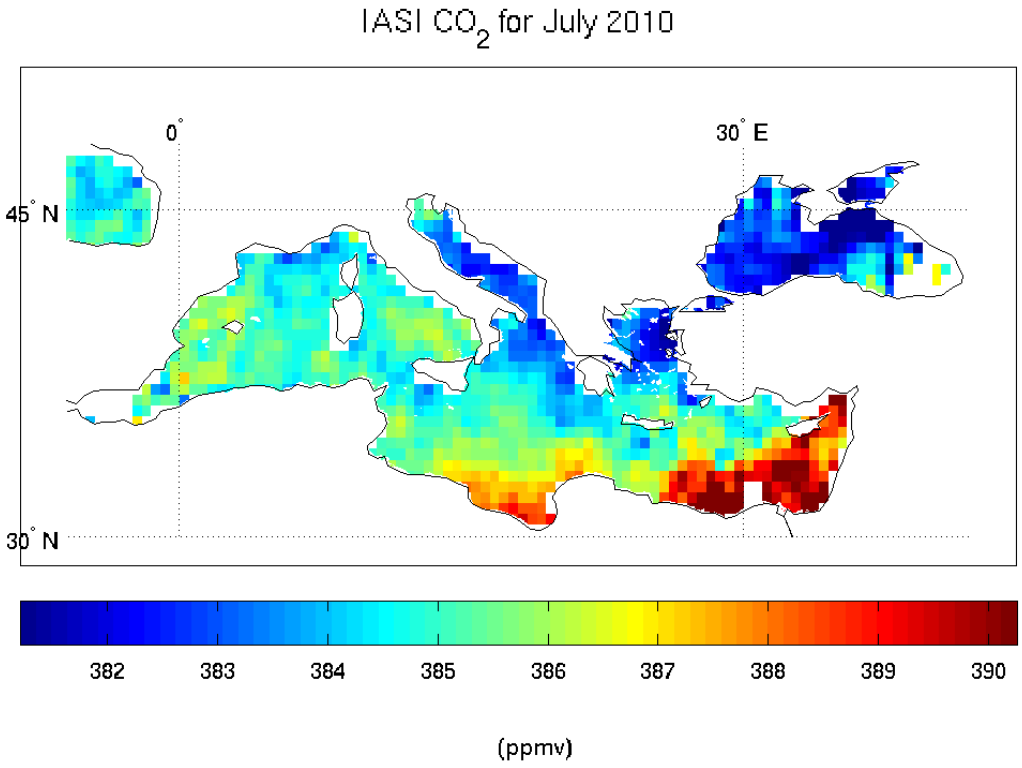

Figure 3. Monthly averages for CO_2 tropospheric content from IASI retrieval.

From figure 3 we can see that there is not an homogeneous distribution of CO2 in the Mediterranean area. There is a clear north-westward gradient of the concentration which is overlapped by other small scale features. In particular, there is a high concentration of the gas in the south-eastern part of the basin. From figure 2 we can see that there are few available measurements in this area.

This could lead us to the conclusion that what we see is the effect of a special event of high CO2 concentration that could have occurred in that part of the basin and that a specular event could have occurred over the Black Sea during the month. This fact should be further investigated. Anyway, the available measurements in the middle of the basin are enough to affirm that there is a strong northward component of the gradient of a few ppmv (3-4) from the Tyrrhenian basin towards the Adriatic basin and that the same occurs in the Aegean Sea. Furthermore, this gradient is observed also at the ground stations. Table 2 shows the monthly averages at the stations and the monthly averages retrieved from IASI around the stations.

Table 2. Monthly averages from ground based measurements and from IASI retrieval of CO_2 concentration. The stations are ordered in an south-eastward direction.

Station	**Ground measurements (*ppmv*)**	**IASI retrieval (*ppmv*)**
Begur	385.67	382.49
Lampedusa	385.73	386.81
Finokalia	383.5	386.37
Cairo	386.8	392.06

The gradient is much more marked in the IASI retrieval than in the ground based measurements but the trend is exactly the same. The local minimum observed in Finokalia is evident also in the IASI retrieved field (the small blue spot southward than Crete Island). The physical reasons for this strong difference in the gradient magnitude maybe due to the fact that the boundary layer is a turbulent part of the atmosphere, therefore, the concentrations tends to be homogenized with respect to the free troposphere.

3.2. CH_4

Methane has the second largest RF of the LLGHGs after CO2 (IPCC 4th Assessment Report: Climate Change 2007). In 2005, the global average abundance of CH4 measured by the network of 40 surface air flask sampling sites operated by NOAA/GMD in both the hemispheres was 1,774.62 ± 1.22 ppbv whilst the pre-industrial concentration estimated from ice core measurements was about 750 ± 4 ppbv in 1750. Its growth rate has decreased form 1% yr-1 in the late 1970s and early 1980s to zero at the end of 1990s. The reasons for the decrease of the atmospheric CH4 growth rate are not understood but are clearly related to changes in the imbalance between CH4 sources and sinks. The sources of atmospheric CH4 are mostly biogenic and include wetlands, rice agriculture, biomass burning and ruminant animals.

Methane is also emitted by various industrial sources including fossil fuel mining and distribution.

Figure 4 shows the monthly averaged CH4 atmospheric concentration over the Mediterranean basin after the same filtering tool used for figure 3.

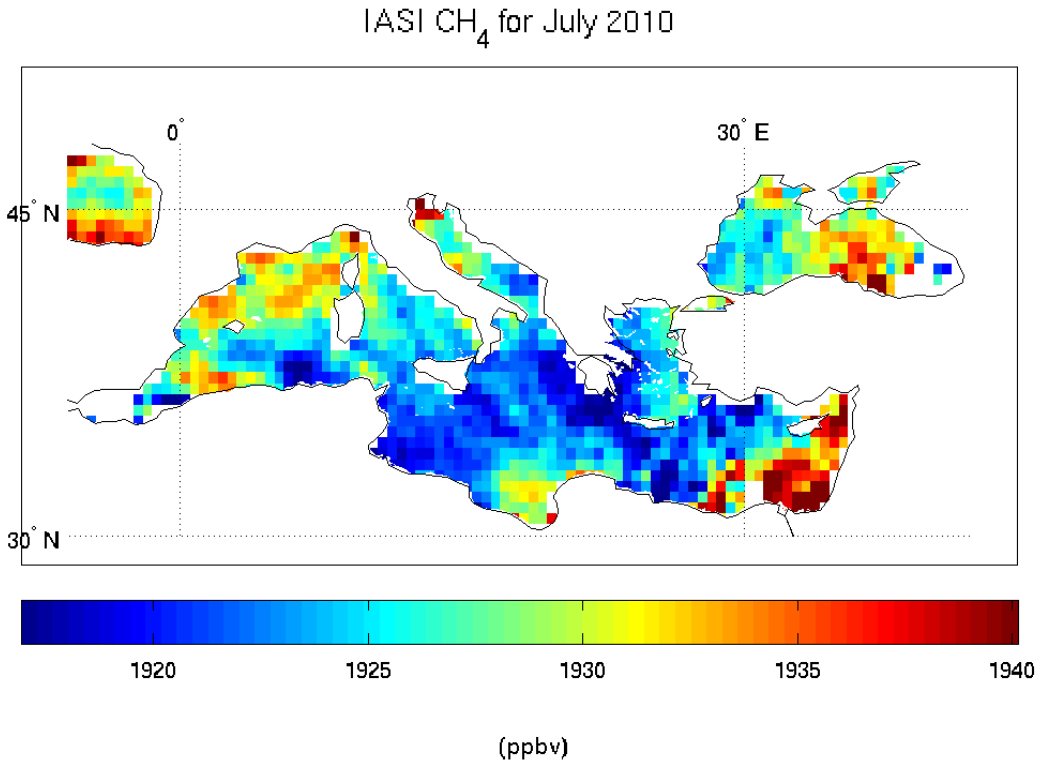

Figure 4. Monthly averages for CH_4 tropospheric content from IASI retrieval.

Figure 3 shows a different trend with respect to the CO2 concentration. Here it seems that we have rather a parabolic trend in the northwest-southeast direction. Once more we have to remark that the eastern part of the basin has few samples and this effect maybe rather representative of a peak event. In the most sampled area we register a minimum in the Aegean Sea and a maximum in the Ligure-Provencal basin which extends partly in the Tyrrhenian Sea.

Table 3 shows the averaged ground measurements and the averaged retrieved values for the CH4 concentrations on 4 of the 5 selected GAW stations.

The first evident feature is that the retrieved values are sensibly higher than the ground based measurements. This feature is quite expected. It would be the same value if the profile was constant with altitude, but that's not the case. The retrieval is not sensible to the boundary layer and is instead representative of the tropospheric concentration of the gas.

On the other hand, the geographical trend is the same. Here, the situation is opposite than for CO2. The intensity of the gradient is much stronger for the ground measurements than for the retrieval. In fact, the retrieved values range in an interval of 20 ppbv whilst the ground based measurements range in an interval of more than 50 ppbv. As said before, the Ligure-Provencal basin is an area of local maximum for the concentration of CH4. Anyway, if we carefully look at figure 4, the only small blue spot is exactly around Begur and this is confirmed also by ground based measurements. This gives an idea of the performance of the retrieval from the point of view of the geographical resolution.

Table 3. Monthly averages from ground based measurements and from IASI retrieval of CH_4 concentration. The stations are ordered in an south-eastward direction.

Station	Ground measurements (*ppbv*)	IASI retrieval (*ppbv*)
Begur	1833.95	1920.14
Lampedusa	1859.84	1923.56
Finokalia	1864.7	1930.13
Sede Boker	1889.65	1936.32

3.3. N_2O

N2O is a powerful GHG with a lifetime of about 114 yr. Its global potential warming (GWP) is 298 time higher than CO2. Its mean mixing ratio in Lampedusa during 2008 was 322.5 ppbv and its annual growth rate is estimated to be 0.78 ppbv yr-1 with a linear trend. The agreement of recorded data in Lampedusa with the global data reported by the IPCC, 2007 makes this site a good proxy to monitor the concentration of N2O both on global and regional scales (Artuso et al., 2010 [12]).

It is the major source of NO to the stratosphere and with the considerable reduction of CFCs in the atmosphere thanks to the Montreal protocol, it is the dominant ozone-depleting substance emitted in the 21st century (Ravishankara et al. 2009 [13]).

N2O is produced both naturally and anthropogenically. The anthropogenic activity includes the use of ammonium fertilizers in agriculture, the fuel combustion, the adipic and nitric acid industrial production and the waste management activities (Cicerone, 1989 [14]). The natural processes which influence the N2O tropospheric concentration are of biological and abiotic nature. Natural microbial production accounts for about 2/3 of N2O emissions. Among the abiotic processes we mention, the seasonal ingassing and outgassing of cooling and warming surface waters which creates a thermal signal in the tropospheric N2O (Nevison et al., 2011 [15]).

Figure 5 shows the average N2O tropospheric concentration for the month of July. The original field has been filtered with the Wiener filter exactly as done for CO2 and for CH4.

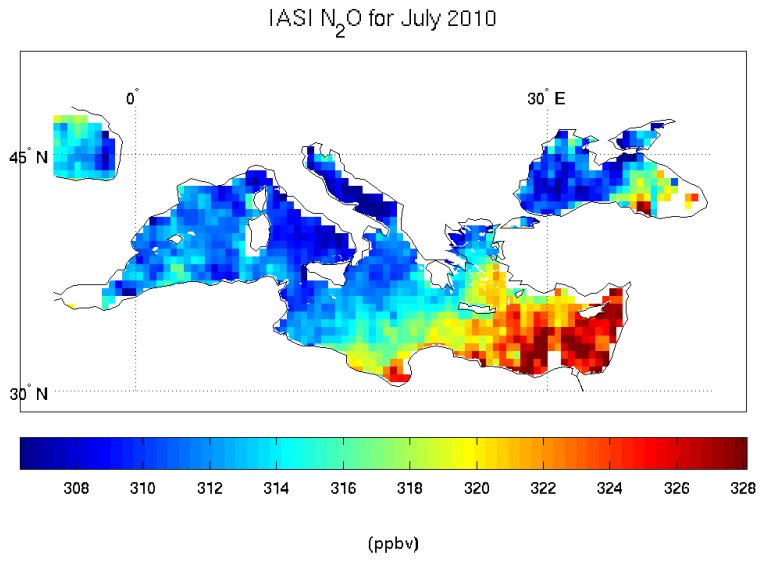

Figure 5. Monthly averages for CH4 tropospheric content from IASI retrieval.

Figure 5 shows a very well marked north-westward gradient which is partly in agreement with the CO2 trend. All figures 3 to 5 confirm that the south eastern part of the basin is the most polluted one. Once more we remark that the phenomenon may be caused by a down sampling of the area, but as in the case of CO2 and CH4, the N2O gradient is confirmed also in the central part of the basin, where the available IASI measurements are copious.

The only station with available ground based measurements is the ENEA station located in Lampedusa. The monthly averaged retrieved value is 309 ppbv whilst the ground based averaged measurement is 323 ppbv. This disagreement is expected, as in the case of all trace gases which does not have a constant vertical profile. The retrieval is sensible to the N2O concentration between 800 and 200 mb, therefore it misses all signal from the lowest atmospheric layers. We know that a higher concentration in the boundary layer with respect to the free troposphere is compatible with real observed data. Let's consider the following two figures (7 and 8). They show the distribution of aircraft N2O concentration measurements at altitudes between 0 and 2000 m (corresponding approximately to 800 mb) and between 2000 and 8000 m (corresponding approximately to 200 mb) on the area around Japan showed in figure 6 from February 2011 to February 2013 (Data have been acquired by the Japanese Meteorological Agency). The average values of the two distribution are respectively 320 ppbv and 314.8 ppbv.

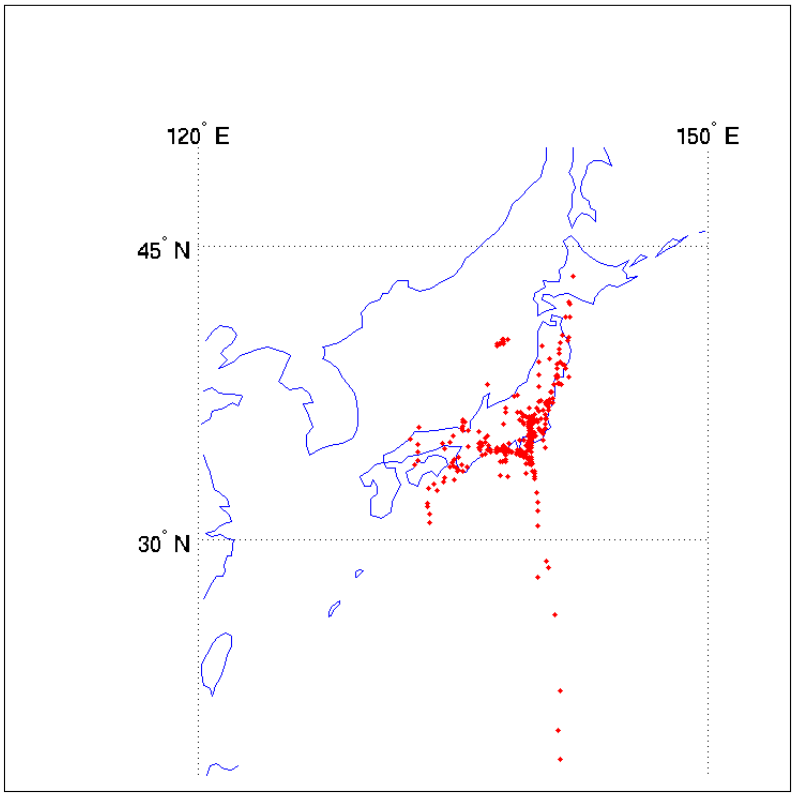

Figure 6. Airplane geographic position during the acquisition of N_2O samples from February 2011 to February 2013 (http://ds.data.jma.go.jp/gmd/wdcgg/wdcgg.html).

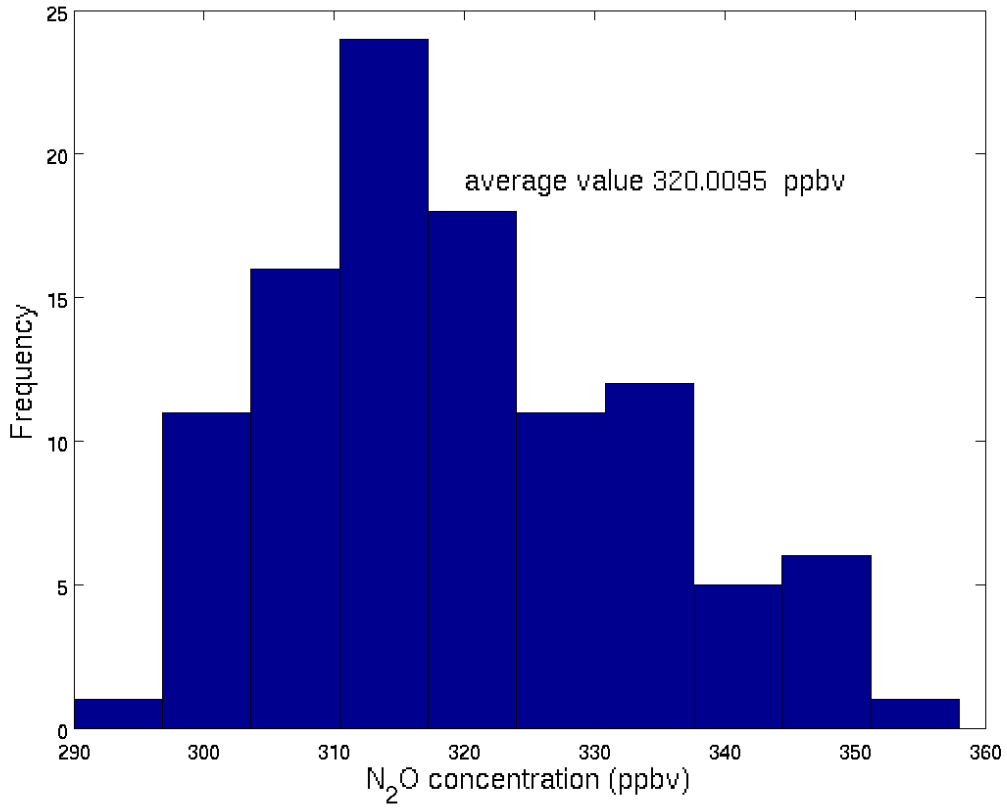

Figure 7. Distribution of aircraft measurements at altitudes between 0 and 2000 m on an area around Japan between February 2011 and February 2013 (http://ds.data.jma.go.jp/gmd/wdcgg/wdcgg.html)

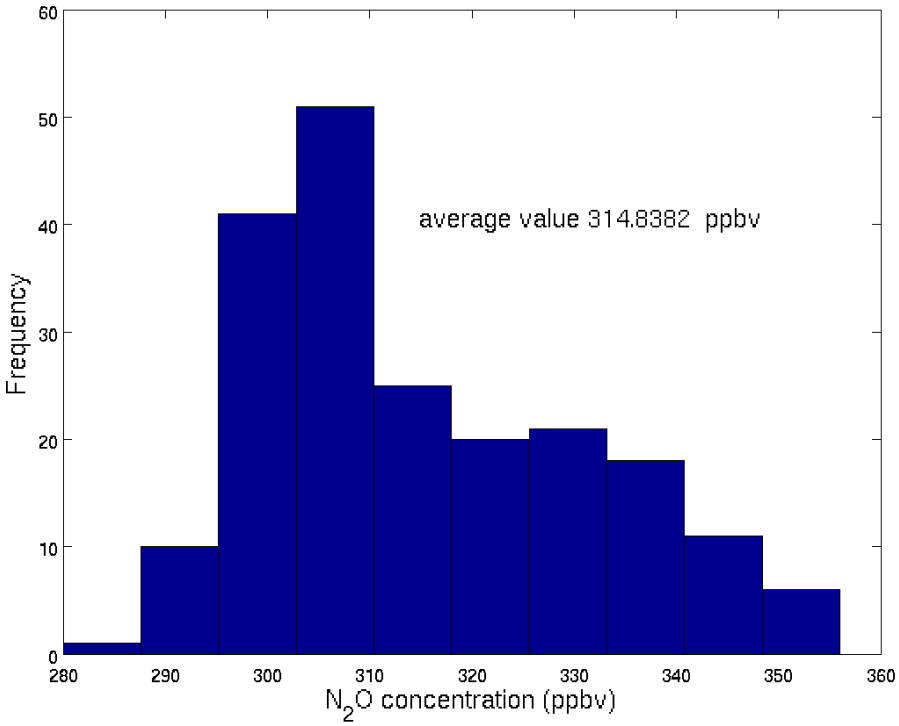

Figure 8. Distribution of aircraft measurements at altitudes between 2000 and 8000 m on an area around Japan between February 2011 and February 2013 (http://ds.data.jma.go.jp/gmd/wdcgg/wdcgg.html)

It's important to stress that the most of atmospheric sources of N2O are located at the surface. As previously said, the biological emission of N2O accounts for 2/3 of the total emissions and that all the anthropogenic sources are also located at the surface. Therefore, its plausible that the concentration of N2O is higher at the surface than in the rest of the troposphere where the gas is in part destroyed.

3.4. CO

CO is not considered a proper greenhouse gas but it has a strong indirect influence on the atmospheric radiative balance. The most important source of CO is the biomass burning and the fossil fuel combustion. Almost the half of the total burden of CO comes from the oxidation of CH4 and non-methane hydrocarbons (NMHC), like isoprene. Vegetation and oceans are considered sources of secondary importance. On the other side, around the 90% of CO is destroyed by reaction with the hydroxyl (OH) radical and the remaining 10% is captured by soils (Brenninkmeijer and Novelli, 2003 [16]). CO has a strong influence on the lifetimes of LLGHG because of its reaction with OH. Furthermore, CO and CH4 oxidation is partially responsible of the production and destruction of tropospheric ozone. It has a lifetime of 1-2 months, therefore it is considered a good tracer to study the tropospheric transport of pollution (Logan et al., 1981 [17]).

Figure 9 shows the monthly average of CO concentration over the Mediterranean basin for the month of July after the application of a low pass filtering tool as done for the other trace gases we previously dealt with.

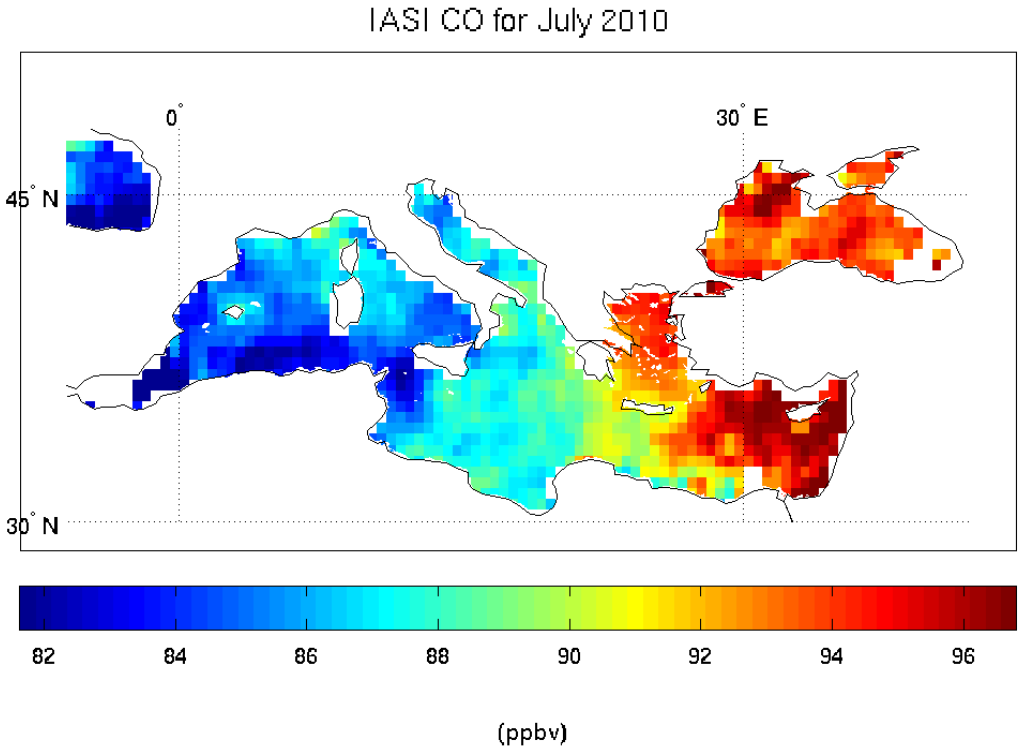

Figure 9. Monthly averages for CH_4 tropospheric content from IASI retrieval.

The monthly averaged CO field has characteristics similar to the other averaged trace gases fields (fig. 3, 4 and 5). The westward gradient of CO concentration is very well marked. The absolute maximum is located in the south-eastern part of the basin, as for the other trace gases, but a local maximum is well distinguishable in the Ligure-Provencal basin. Once more, we cannot be sure of the high concentration recorded in the extreme eastern part of the basin because of the low amount of available satellite measurements, but the gradient is the same (both in direction and intensity) in the better sampled central area of the basin.

The monthly averaged retrieved concentration is 85 ppbv in Lampedusa and 96 ppbv in Sede Boker, where the monthly averaged ground measurements are respectively 121 and 140 ppbv. The difference is around 40 ppbv for both the stations. This large difference is due to the fact that the retrieved values refer to the tropospheric content of the gas (atmosphere between 700-800 and 200 mb). This difference is expected because we do not expect the vertical profile of CO is constant with altitude. The experimental measurements acquired by the MOZAIC (Measurements of OZone water vapour, carbon monoxide and nitrogen oxides by in-service AIrbus airCraft) experiment confirm this trend. Klonecky et al. 2012 [18] concentrate their analysis on the period from May to December 2008 mainly in the north Atlantic area. They show that CO has a monthly average concentration of around 130 ppbv in the atmospheric layer comprised between 1050 and 800 mb and a concentration of around 90-100 ppbv in the layers between 800 and 300 mb, the part of the atmosphere where IASI data are mainly sensitive. The difference is of around 30 ppbv and is consistent with the differences that we found in our comparison.

The gradient observed from the retrieved CO concentration seems to be supported by the ground measurements. This fact seems to confirm once more that the eastern part of the Mediterranean works as a collector or a source of pollution. The reasons of this feature should be investigated and go beyond the purposes of this study, but the first impression is that it could be due to the presence of large metropolitan and polluted areas like Cairo and Istambul supported by a general circulation which does not allow the replacement of polluted air with new fresh air. This thesis is supported by a fast look at the brightness temperature frames acquired in the infrared channel at 12 μm by the imaging radiometer SEVIRI onboard the geostationary platform Meteosat 2G for the whole month of July 2010. From these frames it can be seen that the Eastern Mediterranean is often interested by a local high-pressure condition associated with a flux from the Central and Eastern Europe. Kalabokas et al. 2013 [19] show that the highest tropospheric ozone levels recorded in the Eastern Mediterranean occur under high-pressure (anticyclonic) meteorological conditions. These meteorological conditions are also associated with a lower troposphere and boundary layer flow transporting pollutants from the Central and Eastern Europe and/or Balkans towards the Eastern Mediterranean.

3.5. Time performance of the code.

The down-sampling of the layer optical depth database has given a considerable speed-up to the code. Consider that for applications related to IASI, the layer optical depth database has reduced from 2 Gb to 0.5 Gb. Table 4 shows the performance of the code evaluated on a dedicated machine

equipped with 6 physical and 6 virtual intel i7 cores with a clock frequency of the clock processor unit (CPU) of 3.33 GHz and a total RAM memory of 24 Gb.

Table 4. Time performance of the code expressed in seconds evaluated on the whole IASI spectral range (645-2760 cm-1). FR stands for full resolution layer optical depth database, DR for the donw-sampled one, R stands for spectral radiance, JT for Jacobian of temperature, JTS for Jacobian of skin temperature, JH2O for Jacobian of water vapor, JO3 for Jacobian of ozone. ALL stands for all the entities which can be calculated by the code. Apart R, JT, JH2O, JTS and JO3 it includes also the Jacobian of N2O, the Jacobian of CO2, the Jacobian of CO, the Jacobian of methane, the Jacobian of all the not modifiable mixed gases and the three Jacobians of continua coefficients, the self and foreign for water vapor and the foreign for CO2.

	FR (s)	**LR (s)**	**Speed-up**
R	15	.95	15.8
R, JTS, JT, JH_2O, JO_3	41	3.5	11.7
ALL	103	9.3	11.1

The performance has been evaluated on the whole IASI spectral range (645-2760 cm-1) on three different cases which we think are more representative of the possible applications. The first refers to the simple computation of the radiance spectrum, the second is referred to the computation of the spectral radiance and of the Jacobians of skin temperature, temperature, water vapor and ozone profiles and finally, the case where all the possible entities the code can compute are definitely computed. In addition to what stated before, the code can compute the Jacobians of CO2, CO, CH4, N2O, mixed not modifiable gases and self and foreign continua coefficients of water vapor and foreign continuum coefficient of CO2. For all the three combination proposed in table 4, the speed-up is always greater than 10. Furthermore, in absolute terms, the time performance of the new code makes it useful also for operational purposes. Just to have an idea, the average time spent per inversion is around 14 s. In particular, when the number of iterations is just one, the time decreases to around 8 seconds.

This result suggests the obvious conclusion that a good choice of the first guess considerably reduces the computational time. This time seems still too much high for operational purposes if we consider that a sensor like IASI acquires around 90000 spectra per orbit in a time interval of around 1h40m. This means that each spectrum is acquired in around 0.1 seconds and this would seem the reference time for operational purposes. Anyway, not all the acquired spectra may be processed by the inverse radiative transfer tool described in Masiello et al. 2009 [3]. In fact, this method can be applied to only clear sky spectra. As a thumb rule, the clear sky spectra on the whole hemisphere are around 20-30% of the total. If we consider 10 seconds as the average time to retrieve the thermal and humidity state of the atmosphere, a cluster of 50 CPUs like the one used in this application is enough for operational purposes. The use of a physical based methodology to retrieve the thermal and humidity state of the atmosphere would considerably increase the quality of the level 2 products.

The factors responsible of this speed-up may seem obvious but it's worth the way to discuss them briefly. The fact that the size of the layer optical depth database reduces by a factor 4 has multiple implications on the performance of the code. In fact, the first conclusion is that the code makes much less floating point operations. Furthermore, the small size of the new down-sampled database

makes it possible to store all the parameterized optical depth coefficients in the RAM memory. This allows a more efficient use of the Input/output operations with a consequent reduction of the operating system calls and of the interruption of the pipe line of the CPU.

4. Conclusions

A new implementation of the σ-IASI code has been presented. The layer optical depth database has been down sampled and this allows an operational use of the code in order to retrieve the thermodynamic state of the atmosphere and the tropospheric concentration of the trace gases CO, CO2, CH4 and N2O. An application of the code has been proposed: the tropospheric concentration (800-

200 mb) of the above mentioned trace gases has been retrieved for the month of July 2010 by means of a retrieval scheme based on the FTS-PSI technique and the results have been discussed and compared to the ground based measurements coming from the GAW stations which lie in the Mediterranean Basin. The comparison shows that the retrieval is compatible with the typical vertical profiles of the trace gases object of the study.

The monthly averaged fields show that the eastern part of the Mediterranean Basin has a higher concentration of pollutants with respect to the western part. The physical causes of this phenomenon have to be further investigated but the first feeling is that the Mediterranean atmospheric circulation in that period of the year brings pollutants generated by the metropolitan areas of Cairo, Istanbul and in Central , Eastern Europe and in Balkans towards the eastern part of the basin and doesn't allow a renewal with fresh air.

Acknowledgements

The ground based measurements in Lampedusa and Sede Boker have been provided by NOAA/ESRL and have been downloaded from (http://www.esrl.noaa.gov/gmd/dv/iadv/). The ground based measurements in Begur and Finokalia have been provided by Laboratoire des Sciences du Climat et de l'Environnement (http://www.lsce.ipsl.fr/). The ground based measurements in Cairo have been provided by the Egyptian Meteorological Authority (http://ema.gov.eg/). The ground based measurements in Lampedusa for what concerns N2O have been provided by the Italian Agency ENEA. The N2O vertical profiles acquired by mobile aircraft platform have been provide by the Japanese Meteorological Agency and have been downloaded from the WDCGG web site (http://ds.data.jma.go.jp/gmd/wdcgg/wdcgg.html).

References

[1] Aumann, H.H., Chahine, M.T., Gautier, C., Goldberg, M.D., Kalnay, E., McMillin, L.M., Revercomb, H., Rosenkranz, P.W., Smith, W.L., Staelin, D.H., Strow, L.L., and Susskind, J. *Airs/amsu/hsb on the aqua mission: design, science objectives, data products, and processing systems*. Geoscience and Remote Sensing, IEEE Transactions on, 41(2):253-264, feb. 2003.

[2] Cayla F. R. High spectral resolution infrared remote sensing for earth's weather and climate studies. NATO ASI, Series 9, Springer, Berlin, pages 9-19, 1993.

[3] Masiello, G., Serio, C., Carissimo, A., Grieco, G., and Matricardi, M. *Application of φ-iasi to iasi: retrieval products evaluation and radiative transfer consistency*. Atmospheric Chemistry and Physics, 9(22):8771-8783, 2009.

[4] Amato U., Masiello G., Serio C., and Viggiano M. *The σ-iasi code for the calculation of infrared atmospheric radiance and its derivates*. ENVIRONMENTAL MODELLING & SOFTWARE, 2002.

[5] Masiello, G. and Serio, C.. *An effective water vapor self-broadening scheme for look-up-table-based radiative transfer*. In K. P. Schaefer, O. Lado-Bordowsky, A. Comeron, and R. H. Picard, editors, Society of Photo-Optical Instrumentation Engineers (SPIE) Conference Series, volume 4882 of Society of Photo-Optical Instrumentation Engineers(SPIE) Conference Series, pages 52{61, April 2003.

[6] Shepard, A. Clough, Michael, J. Iacono, and Jean-Luc Moncet. *Line-by-line calculations of atmospheric fluxes and cooling rates: Application to water vapor*. Journal of Geophysical Research: Atmospheres,97(D14):15761-15785, 1992.

[7] Anderson, G. P., Clough, S. A., Kneizy, F. X., Chetwynd, J. H., Shettle, E. P. *Afgl atmospheric constituent profiles (0-120 km)*. Technical report, Air Force Geophysics Laboratory, Hanscom Air Force Base, 1986.

[8] Rothman, L.S., Gordon, I.E., Barbe, A., Chris Benner, D., Bernath, P.F., Birk, M., Boudon, V., Brown, L.R., Campargue, A., Champion, J.-P., Chance, K., Coudert, L.H., Dana, V., Devi, V.M., Fally, S., Flaud, J.-M., Gamache, R.R., Goldman, A., Jacquemart, D., Kleiner, I., Lacome, N., La_erty, W.J., Mandin, J.-Y., Massie, S.T., Mikhailenko, S.N., Miller, C.E., Moazzen-Ahmadi, N., Naumenko, O.V., Nikitin, A.V., Orphal, J., Perevalov, V.I., Perrin, A., Predoi-Cross, A., Rinsland, C.P., Rotger, M., Simeckova, M., Smith, M.A.H., Sung, K., Tashkun, S.A., Tennyson, J., Toth, R.A., Vandaele, A.C., and Vander Auwera, J. *The hitran 2008 molecular spectroscopic data-*

base. Journal of Quantitative Spectroscopy and Radiative Transfer, 110(9-10):533-572, 2009. <ce:title>HITRAN</ce:title>.

[9] Grieco, G., Masiello, G., Serio, C., Roderic, L., Jones, and Mead, Mohammed I.. *Infrared atmospheric sounding interferometer correlation interferometry for the retrieval of atmospheric gases: the case of h2o and co2*. Appl. Opt., 50(22):4516-4528, Aug 2011.

[10] Grieco, G., Masiello, G., Serio, C., *Interferometric vs spectral iasi radiances: Effective data-reduction approaches for the satellite sounding of atmospheric thermodynamical parameters*. Remote Sensing, 2(10):2323-2346, 2010.

[11] Lubrano A. M., Masiello, G., Matricardi, M., Serio, C., and Cuomo, V. *Retrieving n2o from nadir-viewing infrared spectrometers.* Tellus B, 56(3):249{261, 2004.

[12] Artuso, F., Chamard, P., Chiavarini, S., di Sarra, A., Meloni, D., Piacentino, S., and Sferlazzo, M.D. *Tropospheric halocompounds and nitrous oxide monitored at a remote site in the mediterranean*. Atmospheric Environment, 44(38):4944-4953, 2010.

[13] Ravishankara. Nitrous oxide (n2o): *The dominant ozone-depleting substance emitted in the 21st century*. Science, 326:123-125, 2009. DOI:10.1126/science.1176985.

[14] Ralph, J. Cicerone. *Analysis of sources and sinks of atmospheric nitrous oxide (n2o)*. Journal of Geophysical Research: Atmospheres, 94(D15):18265-18271, 1989.

[15] Nevison, C. D., Dlugokencky, E., Dutton, G., Elkins, J. W., Fraser, P., Hall, B., Krummel, P. B., Langenfelds, R. L., O'Doherty, S., Prinn, R. G., Steele, L. P., and Weiss, R. F.. *Exploring causes of interannual variability in the seasonal cycles of tropospheric nitrous oxide*. Atmospheric Chemistry and Physics, 11(8):3713-3730, 2011.

[16] Brenninkmeijer, C. A. M. and Novelli, P. C. *Carbon monoxide* in: Encyclopedia of Atmospheric Sciences, volume 1 pg. 2389-2396. Academic Press, an imprint of Elsevier Science, London, UK, 1st edition, 2003.

[17] Logan, Jennifer A., Prather, Michael J., Wofsy, Steven C., and McElroy, Michael B.. *Tropospheric chemistry: A global perspective*. Journal of Geophysical Research: Oceans, 86(C8):7210{7254, 1981.

[18] Klonecki, A., Pommier, M., Clerbaux, C., Ancellet, G., Cammas, J.-P., Coheur, P.-F., Cozic, A., Diskin, G. S., Hadji-Lazaro, J., Hauglustaine, D. A., Hurtmans, D., Khattatov, B., Lamarque, J.-F., Law, K. S., Nedelec, P., Paris, J.-D., Podolske, J. R., Prunet, P., Schlager, H., Szopa, S., and Turquety, S. *Assimilation of iasi satellite co fields into a global chemistry transport model for validation against aircraft measurements*. Atmospheric Chemistry and Physics, 12(10):4493–4512, 2012.

[19] Kalabokas, P. D., Cammas, J.-P., Thouret, V., Volz-Thomas, A., Boulanger, D., and Repapis, C. C. *Examination of the atmospheric conditions associated with high and low summer ozone levels in the lower troposphere over the eastern mediterranean.* Atmospheric Chemistry and Physics Discussions, 13(1):2457–2491, 2013.

[20] Amato, U., Carfora, M.F., Cuomo, V., and Serio, C.: *Objective algorithms for the aerosol problem*, Appl. Opt. 34, 5442-5452 (1995) http://www.opticsinfobase.org/ao/abstract.cfm?URI=ao-34-24-5442

[21] Amato, U.; De Canditiis, D.; Serio, C. (1998*). Effect of apodization on the retrieval of geophysical parameters from Fourier-Transform Spectrometers*. Appl. Opt., 37, 6537-6543.

[22] Masiello, G., Serio, C.: *Dimensionality reduction approach to the thermal radiative transfer equation inverse problem*. Geophys. Res. Lett., 31, L11105, 2004. doi:10.1029/2004GL019845.

[23] Carissimo, A., De Feis, I.; Serio, C. (2005). *The physical retrieval methodology for IASI: the δ-IASI code*. Environ. Model. Software, 20, 1111-1126.

[24] Grieco, G., Masiello, G., Matricardi, M., Serio, C., Summa, D., Cuomo, V. (2007). *Demonstration and validation of the φ-IASI inversion scheme with NAST-I data*, Q. J. R. Meteorol. Soc., 133, 217-232.

[25] Masiello, G., Matricardi, M., Serio, C., (2011). *The use of IASI data to identify systematic errors in the ECMWF forecasts of temperature in the upper stratosphere*. Atmos. Chem. Phys., 11, 1009-1021, doi:10.5194/acp-11-1009-2011.

[26] Masiello, G., Serio, C., Antonelli, P. *Inversion for atmospheric thermodynamical parameters of IASI data in the principal components space*. Quarterly Journal of the Royal Meteorological Society, 138, 103-117, 2012. doi:10.1002/qj.909.

[27] Masiello, G., and Serio, C.: *Simultaneous physical retrieval of surface emissivity spectrum and atmospheric parameters from infrared atmospheric sounder interferometer spectral radiances*, Appl. Opt. 52, 2428-2446 (2013) http://www.opticsinfobase.org/ao/abstract.cfm?URI=ao-52-11-2428

[28] Hilton, F., Armante, R., August, T., Barnet, C., Bouchard, A., Camy-Peyret, C., Capelle, V., Clarisse, L., Clerbaux, C., Coheur, P.F., Collard, A., Crevoisier, C., Dufour, G., Edwards, D., Faijan, F., Fourrié, N., Gambacorta, A., Goldberg, M., Guidard, V., Hurtmans, D., Illingworth, S., Jacquinet-Husson, N., Kerzenmacher, T., Klaes, G., Lavanant, L., Masiello, G., Matricardi, M., McNally, A., Newman, S., Pavelin, E., Payan, S., P equignot, E., Peyridieu, S., Phulpin, T., Remedios, J., Schl ussel, P., Serio, C., Strow, L., Stubenrauch, C., Taylor, J., Tobin, D., Wolf, W., Zhou, D.: *Hyperspectral Earth Observation from IASI: four years of accomplishments*. Bullettin of the American Meteorological Society, 93, 347-370, 2012. doi:10.1175/BAMS-D-11-00027.1.

[29] Serio, C., Lubrano, A.M., Romano, F., Shimoda, H. (2000). *Cloud Detection Over Sea Surface by use of Autocorrelation Functions of Upwelling Infrared Spectra in the 800-900-cm^{-1} Window Region*. Appl. Opt. 39, 3565-3572, doi:10.1364/AO.39.003565

[30] Masiello, G., Matricardi, M., Rizzi, R., Serio, C. (2002). *Homomorphism between Cloudy and Clear Spectral Radiance in the 800-900-cm^{-1} Atmospheric Window Region*. Appl. Opt. 41, 965-973. doi:10.1364/AO.41.000965

[31] Masiello, G., Serio, C, Shimoda, H. (2003). *Qualifying IMG tropical spectra for clear sky*. Journal of Quantitative Spectroscopy and Radiative Transfer. 77/2, 131-148. doi:10.1016/S0022-4073(02)00083-3

[32] Masiello, G., Serio, C., Cuomo, V. (2004). *Exploiting Quartz Spectral Signature for the Detection of Cloud-Affected Satellite Infrared Observations over African Desert Areas*. Appl. Opt. 43, 2305-2315. doi:10.1364/AO.43.002305

[33] Masiello, G., Grieco, G., Serio, C., Calbet, X., Stuhlmann, R., Tjemkes, S.: *MTG-IRS correlation interferometry for the retrieval of CO2 columnar amount: An error analysis study*, in: 2011 EUMETSAT Meteorological Satellite Conference, 5-9 September 2011, Oslo, Norway, EUMETSAT P.59, 2011. available online from http://www.eumetsat.int/

[34] Serio, C., Masiello, G., and Grieco, G.: *Fourier Transform Spectroscopy with Partially Scanned Interferograms as a Tool to Retrieve Atmospheric Gases Concentrations from High Spectral Resolution Satellite Observations - Methodological Aspects and Application to IASI*, in: Atmospheric Model Applications, Dr. Ismail Yucel (Ed.), InTech, 248-272, 2012. Available online from: http://www.intechopen.com/